Manar Lo. Dayekh [1]
Saleem A. Hussain [2]
Amin Ghadi [1]

[1] *Department of Atomic and Molecular Physics, Faculty of Basic Sciences, University of Mazandaran, Mazandaran, IRAN*
[2] *Department of Physics, College of Education, Al-Qadisiyah University, Qadisiyah, IRAQ*

Morphological, Topographic, Linear and Nonlinear Properties of Cobalt Oxide Thin Films Prepared by Pulsed-Laser Deposition

In this study, cobalt oxide (CoO) thin films were prepared by pulsed-laser deposition method using a pulsed Nd:YAG laser. The surface morphology of the prepared CoO thin films was uniform with an increase in grain size and the presence of distinctive shapes. The results of the nonlinear optics study demonstrated that the CoO thin films have a saturated nonlinear absorption coefficient, a negative refraction index (self-defocusing), moreover the calculation of third order nonlinearity susceptibility. Thus, CoO thin films possess good properties for the applications of nonlinear optics.

Keywords: Pulsed-laser deposition; Cobalt oxide; Thin films; Nonlinear optical properties
Received: 09 September 2023; **Revised:** 23 November 2023; **Accepted:** 30 November 2023

1. Introduction

In the pulsed-laser deposition (PLD) method, material vapor is deposited as thin film onto substrate [1]. Rising the temperature of target material makes the laser useful for deposition of uniform thin layers. Because of the laser pulses, identical evaporation of the target material occurs regardless the vaporization points of its constituent elements and compounds [2], so, the laser beam is effective when its energy is high enough to react with and vaporize these constituents, and move throughout plasma plume and deposit on the substrate [3]. Parameters such as laser power density, pulse repetition rate, pressure, and target-substrate distance affect this process [4-6]. Pulsed-laser deposition produces high-purity thin films mainly because the laser device is outside the deposition chamber, reducing vacuum chamber impurities. The laser can be used in many experiments for multiple targets, and to prepare multiple thin films fast. This approach also maintains reactant mass [7]. Due to their many applications in electronics and sensing [8,9], catalysts [10], and biomedical devices [11-13].

Cobalt oxides have given attention in recent years. This attention is primarily due to the exceptional properties exhibited by such oxides, including high saturation magnetization [14,15], stable catalytic activity [16-18], and excellent electrochemical performance. Cobalt and cobalt oxide films have been fabricated using several techniques, such as spray pyrolysis [19,20], electron-beam evaporation [21], sol-gel approach [22], reactive sputtering [23-26], and more recently chemical vapor deposition (CVD) [17].

The study of nonlinear optics can expand the understanding of the fundamental nonlinear optics. Therefore, it could be developed and worked on to be better suited for practical applications in a variety of technical fields, such as optical communications, optical storage devices, optical power limiting, optical switchers, and optoelectronic and photonic devices [27-30].

Nonlinear optical properties of the material are measured by using a variety of approaches. The simplest way to assess the properties stated in its great sensitivity to a single laser beam is to use the Z-scan technique [31]. The magnitude and sign of nonlinear properties had been measured utilizing the Z-scan [32]. It also has been utilized to determine the nonlinear optical properties of liquid crystals, organic or carbon-based molecules, dielectrics, and semiconductors [33,34].

The Z-scan operates on the premise the sample is transferred in the Z-direction through the focal point of the Gaussian beam. As the sample travels, so does the way the medium interacts with the laser light. This is due to the fact that the light beam intensity varies depending on the position (z) of the sample in relation to the focus (z=0) [32]. Typically, the sample is placed at the focus of the lens and moved continuously along the z-axis at a distance of z_0 where z is the Rayleigh length [33]:

$$z_0 = \frac{\omega_\circ^2}{\lambda}\pi \qquad (1)$$

where λ represents the wavelength, $\omega_\circ$ is the radius of the laser beam

The Z-scan technique includes using close aperture and open aperture. When measuring nonlinear absorption, the open aperture Z-scan is utilized, whereas when measuring nonlinear refraction, the tight aperture Z-scan is followed [29].

The difference between the highest and minimum magnitude of the normalized transmittance (ΔT) is proportional to the nonlinear phase shift ($\Delta\Phi_0$) [27]. This difference is a frequent indicator of nonlinearity.

$$\Delta T_{p-v} = 0.406\left|\Delta\Phi_0\right| \quad (2)$$

where 0.406 is a constant quantity and

$$\Delta\Phi_0 = k\, n_2\, I_0\, L_{eff} \quad (3)$$

Here, $\Delta\Phi_0$ is the nonlinear phase shift, where k represents the wavenumber [33] and I_0 represents the initial laser beam intensity at focus z=0

$$I_0 = P/\, 2\pi w_\circ^{\,2} \quad (4)$$

where w_0 is the laser beam radius, P its power, and L_{eff} is the sample's effective thickness [33], which is given by

$$L_{eff} = (1 - exp^{-\alpha t}/\alpha) \quad (5)$$

The nonlinear refractive index (n_2) is determined by the following equation:

$$n_2 = \Delta\Phi\, /\, k\, I_0\, L_{eff} \quad (6)$$

The relationship between the change in nonlinear refractive index (Δn) and laser beam intensity (I_0) is given as follows:

$$\Delta n = n_2\, I_0 \quad (7)$$

The nonlinear absorption coefficient can be counted from the open aperture curve utilizing the following formula [34]:

$$\beta = \frac{2\sqrt{2}}{I_0 L_{eff}}\Delta T \quad (8)$$

where ΔT is the single peak or single valley on the Z-scan curve with an open aperture

According to the following relationships (9 and 10), the real and imagery components of the third order nonlinear optical susceptibility ($\chi^{(3)}$) were clarified as nonlinear refraction index and nonlinear absorption coefficient, respectively [33]

$$Re[\chi^{(3)}]\ (esu) = 10^{-4}\,\frac{\varepsilon_0 c^2 n_\circ^2 n_2}{\pi}\quad (cm^2/W) \quad (9)$$

$$Im[\chi^{(3)}]\ (esu) = 10^{-2}\,\frac{\varepsilon_0 c^2 n_\circ^2 \lambda\beta}{4\pi^2}\quad (cm^2/W) \quad (10)$$

The following relation could be utilized to express the absolute value of the third-order nonlinear optical susceptibility $|\chi^{(3)}|$:

$$|\chi^{(3)}| = [Re(\chi^{(3)}) + Im(\chi^{(3)})]^{1/2} \quad (11)$$

In this work, cobalt oxide (CoO) thin films were synthesized by pulsed-laser deposition method on glass substrates using Nd:YAG laser and their nonlinear optical properties were studied.

2. Experimental Work

Cobalt oxide thin films were prepared by pulsed-laser deposition using an Nd:YAG with wavelength of 1064 nm, energy of 1500 mJ and frequency of 6 Hz. The CoO powder was compressed as pellets using a 10 tons hydraulic machine press. Glass substrate was placed opposite to CoO target. The laser beam is applied to the target at 45° angle. The sample is bombarded with laser pulses which form a plume of plasma containing particles of the material to be deposited on the glass substrate. The optical characteristics of CoO thin films have been examined in the wavelength range 300-1100nm using a MEGA-2100 dual-beam UV-Visible spectrophotometer. The nonlinear optical characteristics of these films were determined using Z-scan technique to calculate the nonlinear absorption coefficient and nonlinear refractive index.

3. Results and Discussion

In Fig. (1), the surface morphology of the prepared CoO thin films is shown throughout FE-SEM images with different scales (10µm and 200nm). From these images, the surface morphology of these films is described by homogeneity as well as an increase in the particle size with the presence of distinctive and different shapes (flowers and bushes).

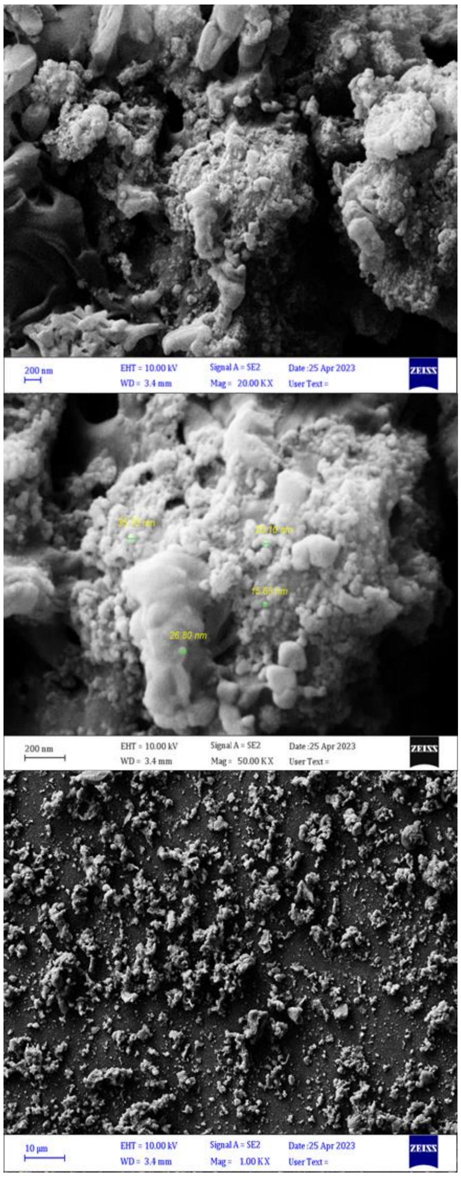

Fig (1) FE-SEM images of the CoO thin films

These images allow to observe that the thin film surface is featured by density and unmistakable increase in the particle size with approximately spherical shape of particles. According to the calculations, CoO thin films typically contain nanoparticles with diameters between 16 and 35nm.

Figures (2) displays the 2D and 3D atomic force microscopy (AFM) images of the prepared CoO thin film deposited on glass substrate. These results indicate that the prepared material exhibit a reasonable degree of homogeneity and uniform vertical heights. Additionally, the results demonstrate an increase in grain size and the absence of voids or cavities on the sample surface. Table (1) illustrates the morphological characteristics of the prepared CoO thin film.

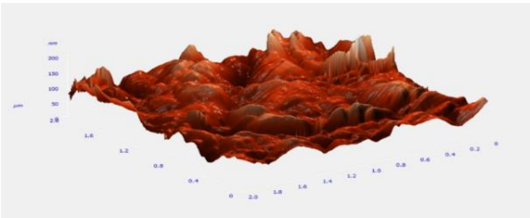

(a)

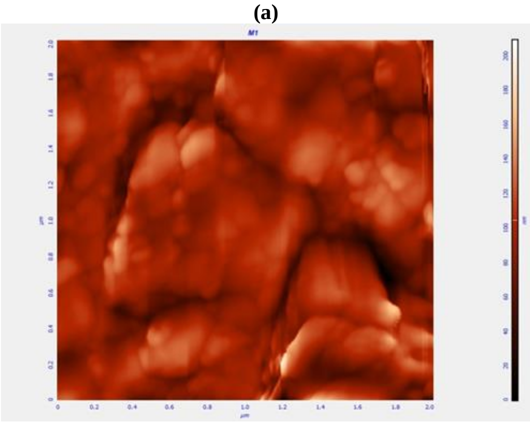

(b)

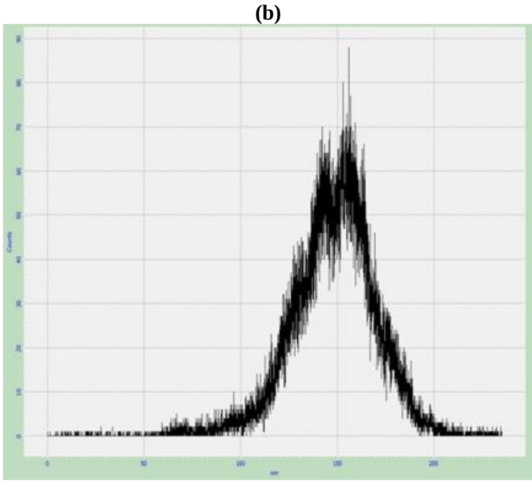

(c)

Fig (2) (a,b) 2D and 3D AFM images of and (c) granular distribution of grains in the CoO thin film

Table (1) Morphological characteristics of CoO samples prepared in this work

Root Mean Square S_q (nm)	Average roughness S_a (nm)
22.0636	16.6863

The optical characteristics of the CoO thin films have been investigated throughout the absorption spectra in the spectral range of 300-1100nm as shown in Fig. (3). The absorption coefficient of the CoO films with thickness of 300nm can be determined by the following relation:

$$\alpha = \frac{2.303A}{t} \qquad (12)$$

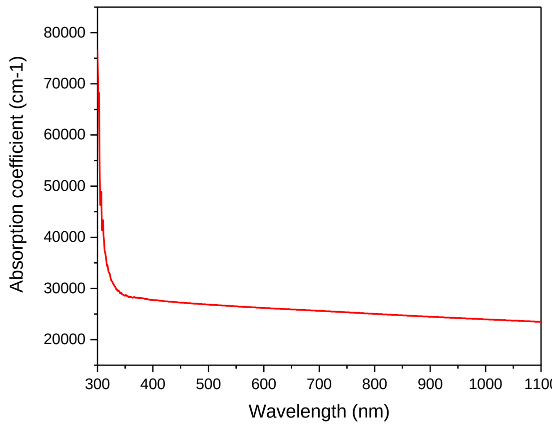

Fig. (3) Wavelength-dependent absorption coefficient of CoO thin films

Figure (4) shows the variation of refractive index of the CoO thin film with wavelength. The refractive index increases with wavelength. It should be seen that the refraction curve is similar to the reflection curve due to the link between reflectance (R) and refractive index (n_0) as

$$n_0 = \frac{1+R}{1-R} + \sqrt{\frac{4R}{(1-R)^2}} - k^2) \qquad (13)$$

The refractive index depends on the crystallization pattern of the material [35,36].

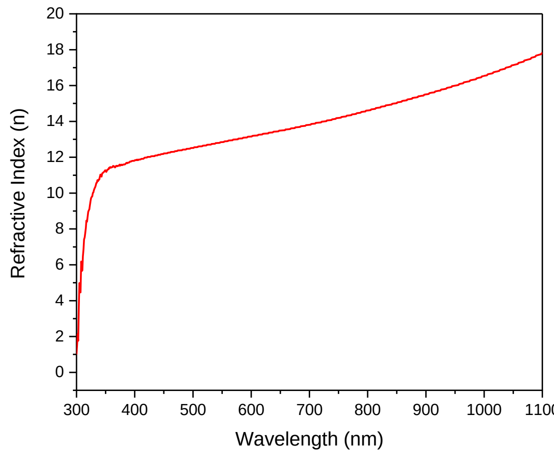

Fig. (4) Relationship of refractive index with wavelength for CoO thin films

Figure (5) depicts the optical conductivity of the CoO thin films prepared in this work. The value of optical conductivity can be estimated using the formula [37]:

$$\sigma = \frac{\alpha n_0 c}{4\pi} \qquad (14)$$

It is evident from this figure that the optical conductivity of CoO film increases with wavelength.

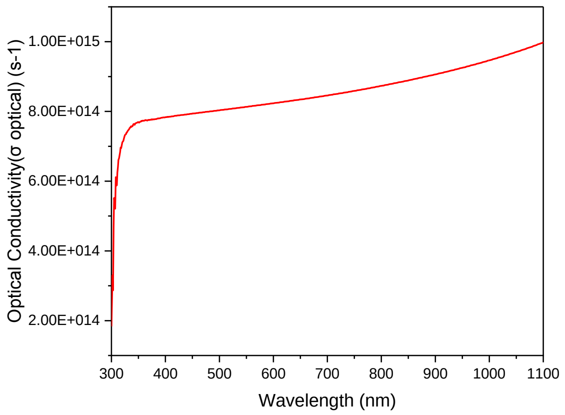

Fig. (5) Optical conductivity vs. wavelength for CoO thin films

Figures (6) and (7) illustrate the results obtained by applying the Z-scan technique on CoO thin films with both close and open apertures using 50mW CW laser diode with wavelength of 650nm. The third-order nonlinear optical susceptibility $|\chi^{(3)}|$ was determined by Eq. (11), the nonlinear absorption coefficient (β) was determined by Eq. (8), the nonlinear refractive index (n_2) was determined by Eq. (6), the change in refractive index (Δn) was determined by Eq. (7), and so forth. The transmission spectrum of CoO thin film was depicted in Fig. (6) at certain location in the close aperture Z-scan setup, while the spectrum illustrated in Fig. (7) was recorded at multiple positions in the open aperture Z-scan setup.

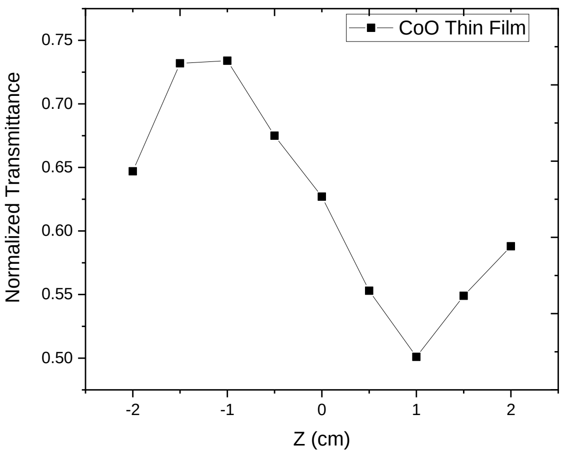

Fig. (6) Normalized transmittance curve of CoO thin film at a 560nm wavelength with 50mW power as a function of position

As explained in figures (6) and (7), the values of transmittance of the CoO thin film to the laser beam in the close-aperture condition are divided by their values in the open-aperture condition to obtain the value of nonlinear refractive index (n_2), which is 1.25×10^{-11} cm^2/mW at 650nm, and the nonlinear absorption coefficient (β) is 1.35×10^{-10} cm/mW at 650nm with power of 50mW, as determined by the Z-scan technique for CoO thin films. According to table (2), the value of third-order nonlinear optical susceptibility $\chi^{(3)}$ at 650nm and power of 50mW is 1.51×10^{-8}.

According to these results, it can be concluded that the prepared CoO thin films have a self-defocusing effect. Also, CoO thin films show high values of the third-order nonlinear optical susceptibility.

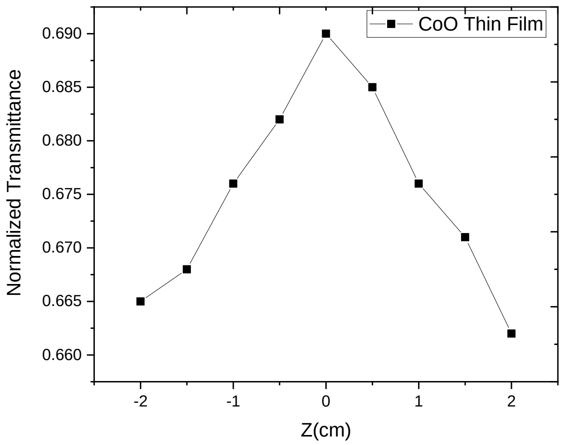

Fig. (7) Normalized transmittance curve of CoO thin film at 560nm with a power of 50 mW as a function of position

4. Conclusion

Cobalt oxide thin films have been prepared by pulsed laser ablation method using a 1064nm Nd:YAG laser. The results showed that the prepared thin films contain nanoparticles with distinctive shapes and diameters of 16-35nm. The surface topography of these films showed homogeneity and uniform vertical heights. The prepared thin films showed that they exhibit self-defocusing refraction and saturated absorption coefficient. Thus these CoO thin films possess good nonlinear properties and can be successfully used in a wide range of optical applications.

References

[1] G.C. Gomes et al., “Nd:YAG (532nm) pulsed laser deposition produces crystalline hydroxyapatite thin coatings at room temperature”, *Surf. Coat. Technol.*, 329 (2017) 174-183.

[2] S.S. Harilal et al., “Internal structure and expansion dynamics of laser ablation plumes into ambient gases”, *J. Appl. Phys.*, 93(5) (2003) 2380-2388.

[3] H. Frey and H.R. Khan (eds.), “**Handbook of Thin Film Technology**”, Springer (Berlin, 2015), 24-44.

[4] H. Fujioka, “**Pulsed Laser Deposition (PLD)**”, in Handbook of Crystal Growth, North-Holland (2015), 365-397.

[5] T. Venkatesan, “Pulsed laser deposition - invention or discovery?”, *J. Phys. D: Appl. Phys.*, 47(3) (2013) 034001.
[6] M. Hashida et al., “Non-thermal ablation of expanded polytetrafluoroethylene with an intense femtosecond-pulse laser”, *Opt. Exp.*, 17(15) (2009) 13116-13121.
[7] A. Ojeda-G-P, M. Döbeli and T. Lippert, “Influence of plume properties on thin film composition in pulsed laser deposition”, *Adv. Mater. Interfac.*, 5(18) (2018) 1701062.
[8] S.C. Tjong and H. Chen, “Nanocrystalline materials and coatings”, *Mater. Sci. Eng. R: Reports*, 45(1-2) (2004) 1-88.
[9] J. Wöllenstein et al., “Cobalt oxide based gas sensors on silicon substrate for operation at low temperatures”, *Sens. Actuat. B: Chem.*, 93(1-3) (2003) 442-448.
[10] P. Haniam et al., “Synthesis of cobalt oxides thin films fractal structures by laser chemical vapor deposition”, *The Sci. World J.*, (2014) Article 685270.
[11] Q. Pankhurst et al., “Applications of magnetic nanoparticles in biomedicine”, *J. Phys. D: Appl. Phys.*, 36(13) (2003) R167.
[12] F.W. Scheller et al., “Thirty years of haemoglobin electrochemistry”, *Adv. Colloid Interface Sci.*, 116(1-3) (2005) 111-120.
[13] O.A. Hammadi, “Using Third-Harmonic Radiation of Nd:YAG Laser to Fabricate High-Quality Microchannels for Biomedical Applications”, *Optik Int. J. Light Electron Opt.*, 208 (2020) 164147.
[14] H.T. Zhu et al., “Synthesis and magnetic properties of antiferromagnetic Co_3O_4 nanoparticles”, *Physica B: Cond. Matter*, 403(18) (2008) 3141-3145.
[15] D.A. Resnick et al., “Magnetic properties of Co_3O_4 nanoparticles mineralized in Listeria innocua Dps”, *J. Appl. Phys.*, 99(8) (2006) Q501.
[16] J. Petryk and E. Kołakowska, “Cobalt oxide catalysts for ammonia oxidation activated with cerium and lanthanum”, *Appl. Catal. B: Enviro.*, 24(2) (2000) 121-128.
[17] X. Wang et al., “One-dimensional arrays of Co_3O_4 nanoparticles: synthesis, characterization, and optical and electrochemical properties”, *The J. Phys. Chem. B*, 108(42) (2004) 16401-16404.
[18] C. Shin et al., “Structural characterization and electrochemical properties of Co_3O_4 anode materials synthesized by a hydrothermal method”, *Nanoscale Res. Lett.*, 7 (2012) 1-7.
[19] L. Guo et al., “Uniform magnetic chains of hollow cobalt mesospheres from one-pot synthesis and their assembly in solution”, *Adv. Func. Mater.*, 17(3) (2007) 425-430.
[20] S.-H. Liu et al., “Graphitically encapsulated cobalt nanocrystal assemblies”, *Chem. Commun.*, 46(26) (2010) 4749-4751.
[21] A.C. Co et al., “Structural and electrochemical studies of Co oxide films formed by the sol-gel technique”, *J. Mater. Sci.*, 40 (2005) 4039-4052.
[22] D. Barreca et al., “Controlled vapor-phase synthesis of cobalt oxide nanomaterials with tuned composition and spatial organization”, *Cryst. Eng. Comm.*, 12(7) (2010) 2185-2197.
[23] O.A. Hammadi and N.E. Naji, “Fabrication and Characterization of Polycrystalline Nickel Cobaltite Nanostructures Prepared by Plasma Sputtering as Gas Sensor”, *Phot. Sen.*, 8(1) (2018) 43-47.
[24] M.A. Hameed, S.H. Faisal, R.H. Turki, “Characterization of Multilayer Highly-Pure Metal Oxide Structures Prepared by DC Reactive Magnetron Sputtering Technique”, Iraqi J. Appl. Phys., 16(4) (2020) 25-30
[25] A.M. Hameed and M.A. Hameed, “Highly-Pure Nanostructured Metal Oxide Multilayer Structure Prepared by DC Reactive Magnetron Sputtering Technique”, Iraqi J. Appl. Phys., 18(4) (2022) 9-14.
[26] A.M. Hameed and M.A. Hameed, “Spectroscopic characteristics of highly pure metal oxide nanostructures prepared by DC reactive magnetron sputtering technique”, Emergent Materials, 6 (2022) 627-633.
[27] H. Ditlbacher et al., “Spectrally coded optical data storage by metal nanoparticles”, *Opt. Lett.*, 25(8) (2000) 563-565.
[28] F.Z. Henari and S. Cassidy, “Non-linear optical properties and all optical switching of Congo red in solution”, *Optik*, 123(8) (2012) 711-714.
[29] O.A. Hamadi, “Induced variation of focal length of the lens stimulated in Nd:YAG laser crystal with optical power pumping”, *Iraqi J. Laser*, 2 (2005).
[30] A.F. Khusnuriyalova et al., “Preparation of cobalt nanoparticles”, *Euro. J. Inorg. Chem.*, 2021(30) (2021) 3023-3047.
[31] S. Pramodini et al., “Studies on third-order optical nonlinearity and power limiting of conducting polymers using the z-scan technique for nonlinear optical applications”, *Laser Phys.*, 24(4) (2014) 045408.
[32] M. Fontalvo et al., “Measurement of nonlinear refractive index of organic materials by z-scan”, *J. Phys.: Conf. Ser.*, 687(1) (2016) 2-4.
[33] S.K. Saadi, A.A. Naimee and S.S. Ahmed, “Third-Order Nonlinear Optical Properties of Spatial Light Modulator”, *Australian J. Basic Appl. Sci.*, 11(7) (2017) 42-48.
[34] B.A.M. Badr, O.A. Hamadi and A.K. Yousif, “Measurement of thermooptic coefficient of semiconductors by single-beam scanning technique”, *Eng. Technol. J.*, 25(5) (2007) 683-689.
[35] Z.S. Mahdi and G.H. Mohammed, “Structural and Optical Properties of GO-doped (TiO_2:MoS_2) Films Prepared by Pulsed Laser

Deposition”, *J. Survey Fisher. Sci.*, 10(3S) (2023) 5658-5668.
[36] O.A. Hammadi and M.S. Edan, “Temperature Dependencies of Refractive Index and Optical Elasticity Coefficient on Lens Induced in Nd:YAG Crystal”, *Iraqi J. Appl. Phys.*, 8(1) (2012) 35-41.
[37] L.J. Tomar et al., “Effect of Preparation Method on Optical and Structural Properties of TiO_2/ZrO_2 Nano composite”, *J. Nanotech. Adv. Mater.*, 2(1) (2014) 27-33.

Table (2) Nonlinear optical properties of CoO thin film by Z-scan technique using 50mW laser power

λ (nm)	$\Delta\emptyset$ (rad)	ΔT_{P-V}	n$\times 10^{-11}$ (cm²/mW)	Δn	T_{max}	$\beta \times 10^{-10}$ (cm/mW)	$\lvert\chi(3)\rvert \times 10^{-8}$
650	0.573892	0.233	1.25	9.97	0.69	1.35	1.51

